



13th World Conference on Earthquake Engineering
Vancouver, B.C., Canada
August 1-6, 2004
Paper No. 287

TIME – FREQUENCY CHARACTERISTICS OF THE 2001 SOUTHERN PERU, MW = 8.4 EARTHQUAKE

Rubén L. BOROSCHEK¹ and Diana COMTE²

SUMMARY

The Civil Engineering Department of the University of Chile, together with international institutions deployed strong motion stations in the northern Chile seismic gap. These networks recorded the June 23, 2001 Mw=8.4 earthquake that occurred in Southern Peru, which is the strongest event in the last 25 years. This earthquake exhibited, at stiff soil sites, in northern Chile relatively large maximum velocities and accelerations although the recording stations are located more than 400 km away from the epicentral region and 200 km from the southern edge of the rupture. Damage to infrastructure was observed in adobe housing and low strength structures. Typical accelerations are in the order of 0.30 g, considerably larger than those expected from typical attenuation formulas if epicentral distances are considered.

Frequency decomposition of the signals using Fourier techniques and the Wavelet Transform are presented. The evolution of the energy, as a function of selected frequency bands, is analyzed. Typical central frequency varies from 3 to 4.8 Hz for horizontal records and 4.5 to 9.5 Hz for vertical records. These frequencies are consistent with records obtained in Chile for thrust type subduction earthquakes, but are much larger than those observed for other focal mechanism solutions. Ninety five percent of the energy of the records is concentrated below 11 Hz. Evolution of energy for bands higher than the average record frequency is relatively smooth, and for low frequency, the energy shows abrupt changes as a function of time. The sudden changes are associated to dominant large amplitude motions observed in most of the records.

To statically characterize the energy evolution with time a smooth three-parameter envelope adjusted for each frequency band is used, therefore, comparison is possible and results could be applied for synthesis studies.

¹ Civil Engineering Department, University of Chile, Blanco Encalada 2002, Tel: (562) 6784372 (562) 6892833, rborosch@ing.uchile.cl

² Geophysics Department, University of Chile, dcomte@dgf.uchile.cl

INTRODUCTION

The Southern Peru Earthquake

The southern Peru region, as well as the whole western margin of South America, is under the subduction process associated to the interaction of the Nazca and the South American plates; this process allows the seismogenic interplate contact to be able to nucleate large earthquakes. Dorbath et al. [1] determined the size of large and large historical earthquakes in Peru, and in the studied region they presented the following sequence: 1513, 1604, 1687, 1784 and 1868 (Table 1). Therefore, the rupture area associated with the 1868 earthquake had been identified as an important seismic gap, before the occurrence of the 2001 southern Peru earthquake (Nishenko, [2]; Dorbath et al., [1], Comte and Pardo, [3]). However, it is important to point out that the mentioned interplate earthquakes are not equivalent in magnitude, and in the associated rupture areas, exhibiting variable modes of rupture.

Table 1 Major Events

Date	Rupture Length (km)	Mw
1582	80	7.5
1604	450	8.7
1687	150(?)	8.0
1715	75	7.5
1784	300	8.4
1868	500	8.8
2001	300	8.4

The south-central Peru segment (12°-19°S) of the subduction zone has ruptured in underthrusting earthquakes this century from north to south in 1974 (Mw=8.0), 1996 (Mw=7.7), 1942 (Mw=7.9-8.2) and 2001 (Mw=8.4). The 1974, 1996, 1942, and 2001 earthquakes have a source duration of 60, 45, 75, and 100 sec respectively, and all initiated with a small pulse of moment release followed by much larger moment release delayed in time. The 1974, 1996, and 2001 earthquakes all show unilateral SSE rupture with the largest pulse of moment release occurring at least 100 km from the mainshock hypocenter (Giovanni et al. [4])

On June 23, 2001, Mw=8.4 the largest world earthquake of the last 25 years affected the southern Peru region rupturing the northern and central part of the previous large earthquake occurring on August 13, 1868, Figure 1a. A detailed analysis of the aftershock sequence was possible due to the deployment of a temporary seismic network along the coast in the Arequipa and Moquegua districts, complementing the Peruvian permanent stations. This network operated during the first weeks after the mainshock and recorded the major aftershocks like the larger one occurring on July 7, 2001, Mw=7.5, that defines the southern limit of the rupture area of the 2001 Peruvian earthquake. Most of the aftershocks show thrusting fault focal mechanisms according to the average convergence direction of the subducting Nazca plate. However, normal faulting events are also present in the aftershock sequence like the one on July 5, 2001, Mw=6.6.

The segment between Ilo and Tacna did not participate in the rupture process of the 2001 southern Peru earthquake. That seems to be equivalent to the 1784 one, and it is not the replication of the 1868 earthquake. Seismicity located near the political Peruvian-Chilean border was reliably determined using the data recorded by the northern Chile permanent network. The occurrence of the 1995 Antofagasta ($M_w=8.0$) and the 2001 southern Peru earthquakes suggests that the probability of having a major earthquake in the northern Chile region increased, considering that the previous large earthquake in this region happened in 1877 ($M_w\sim 9$), and since that time no earthquake with magnitude $M_w>8$ had occurred within the 1877 estimated rupture area (between Arica and Antofagasta). The obtained rupture aftershock area of about 350 km by 100 km is in agreement with what was obtained by Giovanni et al. [4] using relocated aftershocks recorded globally during the first month.

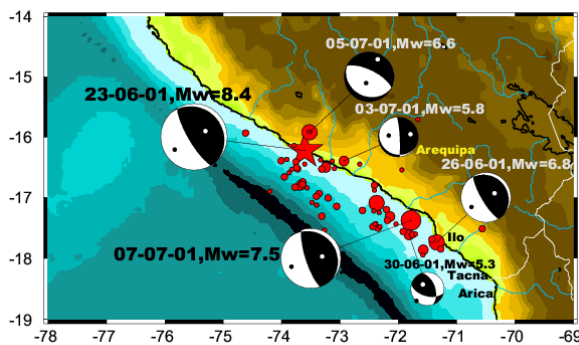


Figure 1a. Distribution of the main aftershocks of the 2001 Peruvian earthquake.

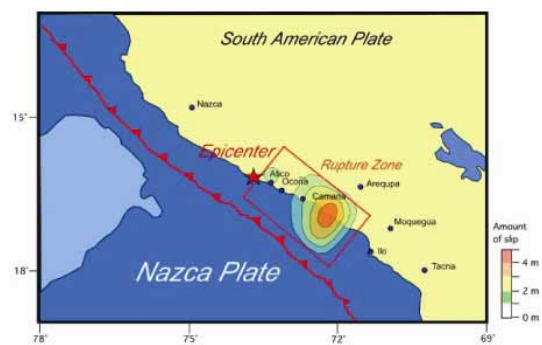


Figure 1b. Source inversion of the teleseismic body-waves of the 2001 southern Peru earthquake (Kikuchi and Yamanaka [5]).

Kikuchi and Yamanaka [5] performed a source inversion of the teleseismic body-waves of the 2001 Peruvian earthquake (Figure 1b) and their general results are in agreement with that obtained by Giovanni et al. [4] modelling the teleseismic broadband P waveforms of the 2001 Peru earthquake and concluded that the source time function has two pulses of moment release with the larger second pulse located approximately 120 to 160 km south-east of the mainshock hypocenter indicating a south-easterly unilateral rupture, which is in agreement with the CMT analysis done by Nettles et al. [6], who also obtained a scalar moment of about $4.95 \cdot 10^{28}$ dyne-cm and a thrust-faulting mechanism with strike, dip and rake of 318° , 14° and 79° , respectively, using a short-period cutoff of 200 s, showing a southward directivity consistent with the southward displacement of the earthquake centroid time shift of 66 s determined by their CMT analysis.

Sladen and Madariaga [7] performed a non-linear inversion of broad-band body waves of the 2001 southern Peru earthquake obtaining that the rupture propagated unilaterally to the south-east with a complicated rupture history of the source time function, that exhibits a broad peak lasting about 50 s and a stronger second peak centered at about 80 s after the initial shock, with the main source of energy (asperity) not located at the hypocenter, but almost 100 km away from

it. They used a similar technique for the three major aftershocks (the $M_w=6.8$ of June 26, the $M_w=6.8$ of July 5 and the $M_w=7.5$ of July 7 events) finding similar thrusting focal mechanisms, but simpler source time associated functions.

GENERAL ACCELERATION RECORD CHARACTERISTICS

The main event was registered by the Department of Civil Engineering Strong Motion Network of the University of Chile (Boroschek et al, [8]), a digital instrument from the Institut de Physique du Globe de Strasbourg located in Arica Hospital and a CISMID strong motion instrument at Moquegua, in Peru. Figure 2 presents the horizontal records obtained. No additional records are known, so most of the records are at a substantial distance from the rupture area. Because of the instrument characteristics, reliable information is in the frequency band between 0.1 to 25 for the analogue instruments and 0.1 to 100 Hz for the digital ones.

The soil characteristics at each Chilean station are still under investigation, but they can be classified initially with an average shear wave velocity between 400 and 600 m/sec for the first 30 meters.

The basic characteristics of the records are presented in Table 2: Maximum acceleration (A_{max}) and velocities (V_{max} , integrated between 0.1 – 25 Hz), strong motion duration from 90% of Arias Intensity (SM Time Arias), root mean square acceleration of the strong phase determined according to Arias Intensity (A_{rms}), strong motion duration from bracket acceleration (SM Time $> 0.05g$), record energy and central frequency for frequencies below 95% of the total energy.

All, with the exception of the Moquegua records are located in the northern part of Chile with an average distance of 450 kilometers from the epicenter and 200 km from Ilo, Peru, the southern most tip of the rupture area. The maximum time amplitudes for this distance are considerable large, but not necessarily uniform. The Moquegua records that are closer to the area of rupture have similar amplitudes. The maximum acceleration in Arica, 0.28, 0.31 and 0.33 g are generally much larger than expected from attenuation formulas obtained in the area for subduction zones if epicentral distance is considered. Also, the duration of the strong motion of around 30 seconds is significantly large.

The velocity observed at 400 kms from the epicenter around 20 cm/sec is consistent with other values observed in other seismic events such as the 1985 Central Zone of Chile magnitude 7.8 event, but no direct comparison is possible due to the lack of information at this distance.

The 5% critical damping linear response spectra for the most severe components are presented in Figures 3 and 4. The elastic response spectra required for the region in the Chilean Seismic Code is also presented in Figure 3. For design the force values obtained with these spectra should be multiply by 1.4, so this event is consistent with expected spectral values. The spectrum at this site has its maximum at a period close to 0.3 seconds and has values higher than 0.1 g up to 3 seconds. The elastic demand of the record was higher than the indicated code demand for

periods above 0.8 seconds. The spectral values obtained in the city of Arica are relative larger than those observed in Moquegua but the period band of higher demands is similar. Additionally, the Moquegua response spectra do not have a defined peak between 0.1 and 0.6 seconds.

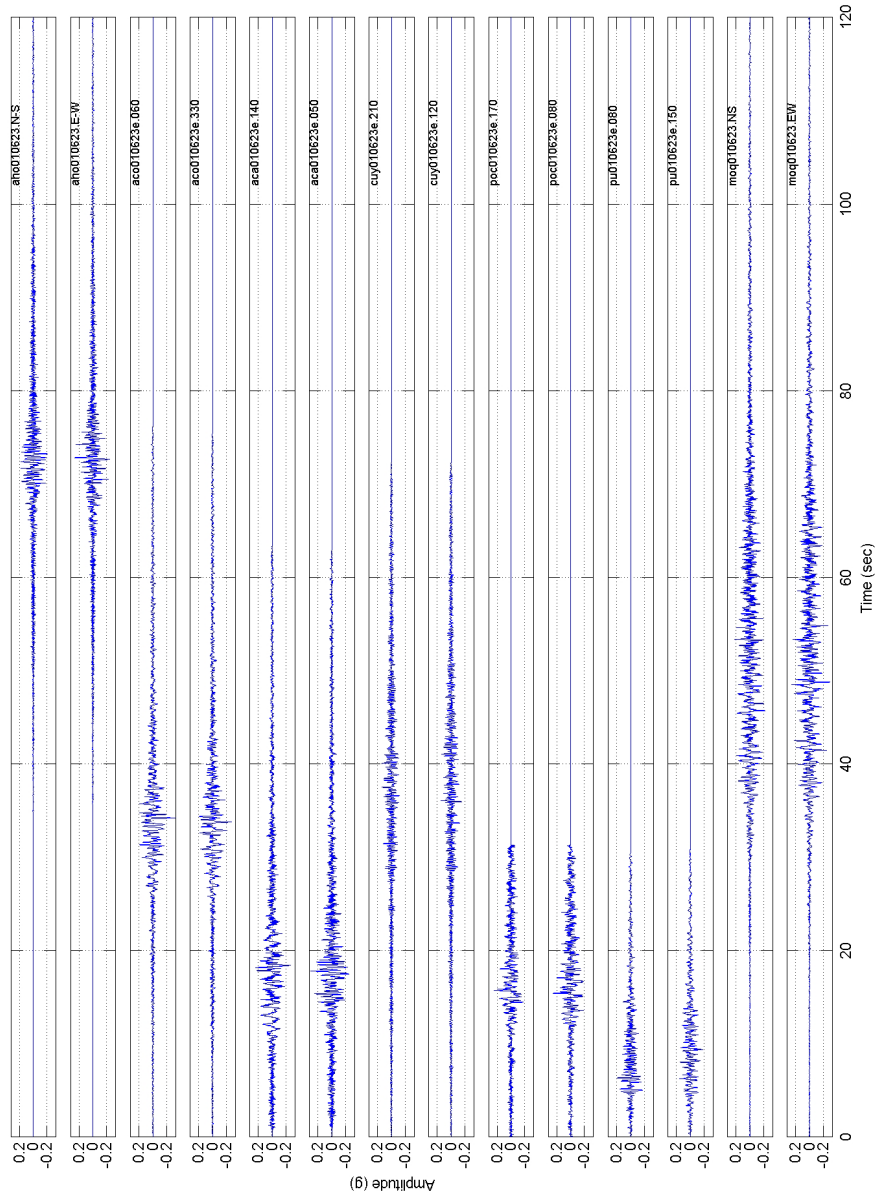


Figure 2. Horizontal time histories.

Table 2. Motion Characteristics

Station	A max	A rms	SM Time	SM Time	Energy	V max	Central
	(g)	(g)	Arias	> 0.05g	(g*g * seg)	(cm/seg)	Frequency
			(seg)	(seg)			(Hz)
Arica Hosp.NS	-0.21	0.05	24.16	22.15	0.07	18.97	4.74
Arica Hosp.EW	0.28	0.05	23.53	23.31	0.07	19.76	4.79
Arica Cost.060	-0.33	0.06	20.40	25.76	0.09	23.96	2.93
Arica Cost.330	-0.28	0.06	22.95	31.17	0.08	19.29	3.15
Arica Casa.140	-0.27	0.06	22.94	30.23	0.09	21.05	3.73
Arica Casa.050	0.31	0.06	23.29	38.78	0.11	22.96	4.34
Cuya.210	0.14	0.03	35.27	24.55	0.04	7.91	4.77
Cuya.120	-0.16	0.04	30.33	27.12	0.05	9.22	4.76
Poconchile.170	0.25	0.05	18.06	23.24	0.05	29.14	4.33
Poconchile.080	0.26	0.06	17.09	23.11	0.07	29.15	3.54
Putre.080	0.20	0.05	14.29	16.42	0.04	10.74	4.16
Putre.150	-0.19	0.05	15.42	16.67	0.04	10.73	3.44
Moquegua NS	-0.22	0.06	36.04	43.50	0.16	29.66	4.08
Moquegua EW	-0.30	0.07	35.85	52.93	0.18	24.80	3.73
Arica Hos.ver	-0.14	0.03	36.01	31.63	0.04	17.07	9.36
Arica Cost.ver	-0.08	0.02	33.10	18.65	0.01	6.79	6.95
Arica Casa.ver	0.18	0.03	29.69	21.92	0.04	12.77	8.14
Cuya.ver	-0.06	0.02	42.76	13.16	0.01	3.85	7.55
Poconchile.ver	-0.14	0.03	24.45	24.73	0.02	14.98	5.72
Putre.ver	0.09	0.02	15.74	8.60	0.01	5.19	4.49
Moquegua.ver	0.17	0.04	38.82	40.90	0.06	0.01	9.52

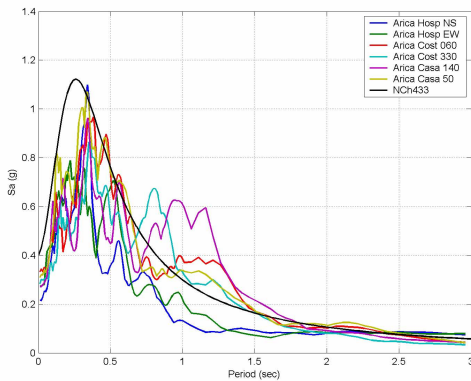


Figure 3. Elastic response spectra for Arica horizontal records and Chilean Code requirements.

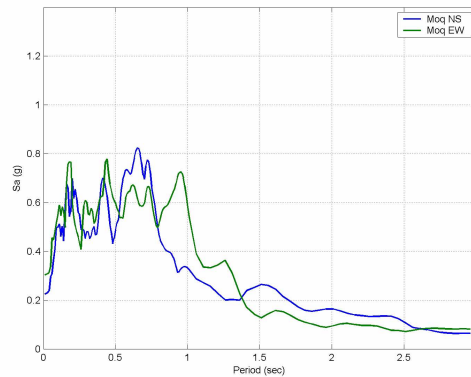


Figure 4. Elastic response spectra for Moquegua records.

The effective acceleration (EPA) derived from the elastic response spectra for the Chilean records indicates a relation of EPA=0.9 PGA which is similar to what was obtained for other seismic events in Chile, (Boroschek, et al, [9] and Comte et al [10]).

The central frequencies were calculated for increasing frequencies from 0 up to the frequency corresponding to 95% of the spectrum energy. As observed from other records in the region, central frequencies are rather large, from 3 to 4.8 Hz for horizontal records and from 4.5 to 9.5 Hz for vertical records. This frequency is generally higher for the records obtained closer to the rupture. The record obtained in Peru, which is even closer, has similar central frequencies but with a broader frequency band. For all the records 95% of the total energy is contained in frequencies below 11 Hz.

TIME - FREQUENCY CHARACTERISTICS

The wavelet transform is used to analyze the time-frequency characteristics of the data set.

The Wavelet Transform

The discrete wavelet transform was developed to detect geologic structure singularities in geophysical seismic refraction studies in the 80's. Later it was further developed by Morlet, Grossmann, Mallat and Daubechies among others, Mallat, [11].

The Discrete Wavelet Transform (DWT) is a projection of the time signal $x(t)$ on the orthonormal basis of functions $\psi_{j,k}(t)$ and $\phi_{j,k}(t)$ called wavelet and scaling function, respectively:

$$d_j(k) = \langle s(t), \psi_{j,k}(t) \rangle = \int_{-\infty}^{\infty} s(t) \psi_{j,k}(t) dt \quad (1)$$

$$c_j(k) = \langle s(t), \phi_{j,k}(t) \rangle = \int_{-\infty}^{\infty} s(t) \phi_{j,k}(t) dt$$

Such that

$$s(t) = \sum_{j=j_0}^J s_j(t) + r_j = \sum_{j=j_0}^J \sum_{k=-\infty}^{\infty} d_j(k) \psi_{j,k}(t) + \sum_{k=-\infty}^{\infty} c_j(k) \phi_j(t) \quad (2)$$

The j and k parameters represent the scale and time variables, respectively. The first term on the right hand side of equation 1 represents the detail description of each scale j and time k . The second term represents the residual signal description after the J level. The Discrete Wavelet Transform (DWT) is an attractive signal processing technique, since fast computation of the wavelet coefficients $d_j(k)$ and $c_j(k)$ is possible thanks to recursive algorithms.

This projection allows the decomposition and analysis at different scales and at different time locations. The wavelets, i.e. functions $\psi_{j,k}(t)$, are recursively developed and consequently they are related to the so-called mother wavelet $\psi(t)$ through the following equation

$$\psi_{j,k}(t) = \frac{1}{\sqrt{2^j}} \psi\left(\frac{t-2^j k}{2^j}\right) \quad (3)$$

There are various wavelet functions with different properties such as Haar, Daubechies, Mexican Hat, etc. However, all the wavelets share the same general properties, i.e $\psi_{j,k}(t)$ are band-pass signals and due to the scaling by factor 2^j their Fourier transform have supports varying with scale parameter j . To illustrate this point, Figure 5 presents the Fourier transforms of functions $\psi_{j,k}(t)$ for $j=0, \dots, 5$ for arbitrary k for the Daubechies wavelet.

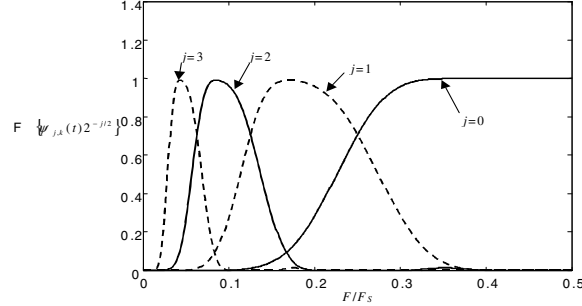


Figure 5. Frequency band equivalence of scale divisions.

Since the wavelets $\psi_{j,k}(t)$ are roughly separated in the frequency domain, so are the signals $s_j(t)$ and consequently, coefficients $d_j(k)$ may be treated as weighting factors corresponding to different frequency bands approximately defined by j :

$$f \in \left[\frac{0.5}{\Delta t 2^{j+1}}, \frac{0.5}{\Delta t 2^j} \right] \quad j = 0, \dots, n-1. \quad (4)$$

However, analyzing Figure 5, it may be observed that these bands are not exactly separated.

The total energy for the signal can be defined as the sum of the energy for each level j and as the square sum of the detail coefficient

$$\sum_t |s(t)|^2 = \sum_{j=0}^J \sum_{k=-\infty}^{\infty} |d_j(k)|^2 + \sum_{k=-\infty}^{\infty} |c_J(k)|^2 \quad (5)$$

So, one may state that varying the coefficients at the scale j , affects the energy content only in the frequency band that corresponds to this scale and only at a time argument defined by coefficient k .

In the present work, due to space limitations, there is no direct work with the detail coefficients. So, the DWT is used to decompose the signal and to estimate the energy evolution with time at each scale. There are other techniques to do this efficiently, Cohen [12], but the advantage of the DWT is that the characteristics determined and parameterized in this form can be easily applied in record synthesis using the inverse wavelet transform. This is not done in this paper, but is indicated in Boroschek, et al [13].

Envelope description

There are several ways to describe the energy evolution in time. In this paper, a relatively smooth envelope, the chi-square distribution modified from the one proposed by Saragoni [14], is used to parameterize the energy evolution for the record and for each scale.

$$\hat{e}_j(t) = E \left\{ |d_j(t)|^2 \right\} = \beta_j e^{-\alpha_j t} t^{\gamma_j} \quad (6)$$

where \hat{e}_j represents the envelope at scale j , and parameters γ and α relate to the first and second time moment of the energy distribution at the j scale. Figure 6 present the Arica Hospital time record and the adjusted parametric envelope.

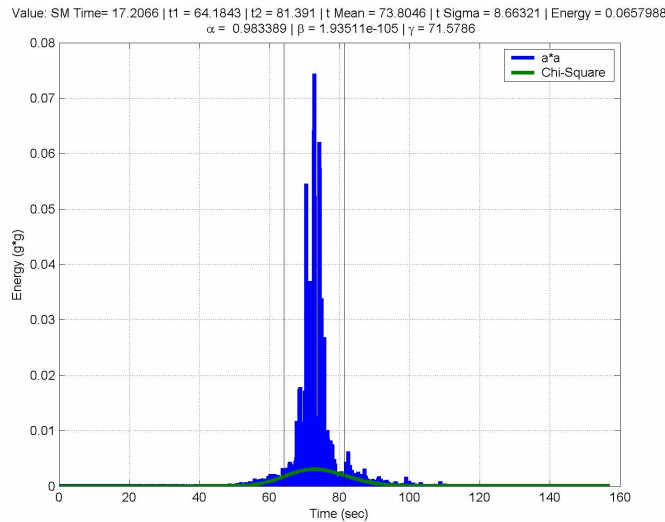
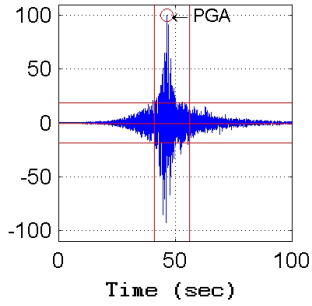


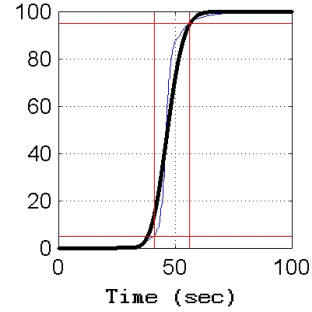
Figure 6. Square acceleration amplitude Arica Horizontal record and adjusted parametric envelope equation.

Using the DWT the records were decomposed and studied in different scales to present their time and frequency evolutions. The decomposition and reconstruction of horizontal EW Arica Hospital and Moquegua EW are shown as examples in Figures 7 and 8, but conclusions are given considering all records studied. These figures have several subfigures: (a) presents the time record, the maximum acceleration, the rms and strong motion duration values; (b) presents the accumulated record energy ($\sum a^2(t)$), and the adjusted parametric equation (eq. 6); (c) presents the percentage of energy of the total record distributed in each scale, (eq 5). The scale can be associated with frequency bands according to Table 3; (d) presents the cumulative energy for each scale and its corresponding parametric adjustment (eq. 5 and 6) and (e) present the table with the scale energy and adjusted parameters.

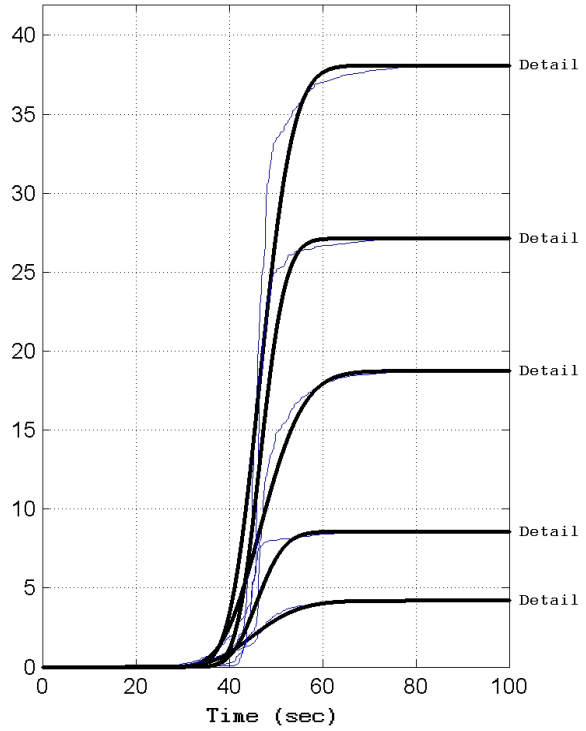
(a) SIGNAL: aho010623.E-W
 PGA = +0.2728 G
 T SM S&H =+17.21 seg
 T SM Arias =+23.67 seg
 T band =+23.31 sec



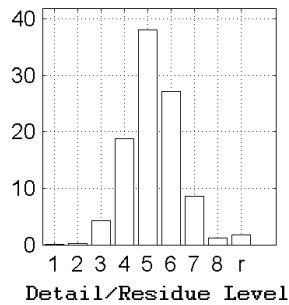
(b) ACUMULATED ENERGY
 α 0.983389 β 1.93511e-105 γ 71.5786



(d) ACUMULATED ENERGY DETAILS
 % Total Energy = 100.00 %



(c) ENERGY DISTRIBUTION
 Total E = 0.065865 G²·seg



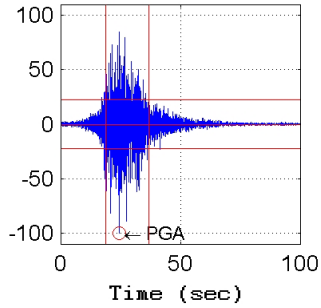
(e) SUMMARY TABLE

LEVEL	FMIN (Hz)	FMAX (Hz)	ENERGY (G ² ·seg)	ENERGY (%)
1	50.00	100.00	1.51E-006	0.002
2	25.00	50.00	1.42E-004	0.216
3	12.50	25.00	2.77E-003	4.199
4	6.25	12.50	1.24E-002	18.756
5	3.13	6.25	2.51E-002	38.128
6	1.56	3.13	1.79E-002	27.157
7	0.78	1.56	5.65E-003	8.576
8	0.39	0.78	8.28E-004	1.257
r	0.00	0.39	1.13E-003	1.708

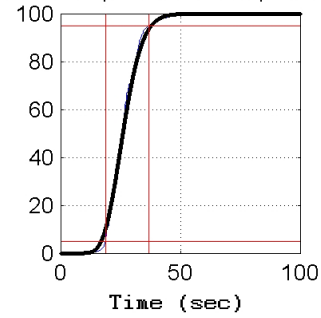
LEVEL	ALPHA (Hz)	BETTA (G ² ·seg)	GAMMA
3	0.510545	+1.60E-055	35.926366
4	0.631883	+4.72E-070	46.164188
5	1.043747	+1.79E-112	76.163003
6	1.768060	+2.33E-188	129.194118
7	1.457055	+2.06E-153	104.856150

Figure 7. Signal decomposition, Arica Hospital record

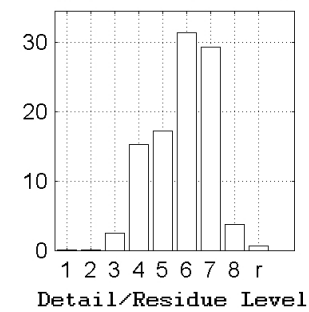
(a) SIGNAL: moq010623.EW
 PGA = -0.3025 G
 T SM S&H =+24.69 seg
 T SM Arias =+35.85 seg
 T band =+52.92 sec



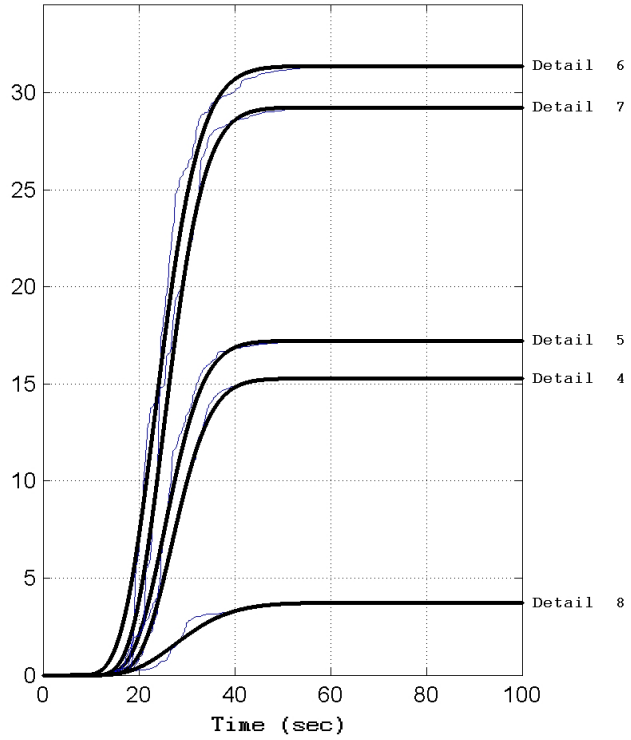
(b) ACUMULATED ENERGY
 α 0.326117 β 2.09811e-023 γ 16.2053



(c) ENERGY DISTRIBUTION
 Total E= 0.184511 G²·seg



(d) ACUMULATED ENERGY DETAILS
 % Total Energy = 100.00 %



(e) SUMMARY TABLE				
LEVEL	FMIN (Hz)	FMAX (Hz)	ENERGY (G ² ·seg)	ENERGY (%)
1	50.00	100.00	2.08E-008	0.000
2	25.00	50.00	3.14E-005	0.017
3	12.50	25.00	4.47E-003	2.423
4	6.25	12.50	2.82E-002	15.298
5	3.13	6.25	3.18E-002	17.240
6	1.56	3.13	5.80E-002	31.420
7	0.78	1.56	5.40E-002	29.283
8	0.39	0.78	6.89E-003	3.735
r	0.00	0.39	1.08E-003	0.584

LEVEL	ALPHA (Hz)	BETTA (G ² ·seg)	GAMMA
4	0.419408	+8.08E-033	22.468801
5	0.395263	+4.55E-029	19.995526
6	0.292794	+3.00E-020	13.611639
7	0.366872	+8.71E-027	18.416646
8	0.215844	+6.82E-020	11.811059

Figure 8. Signal decomposition, Arica Hospital record

Table 3. Approximate Scale - frequency bandwidth relationship

Scale	Lower F (Hz)	Higher F (Hz)
1	50.00	100.00
2	25.00	50.00
3	12.50	25.00
4	6.25	12.50
5	3.13	6.25
6	1.56	3.13
7	0.78	1.56
8	0.39	0.78

Several characteristics can be described from these figures and decompositions:

The cumulative energy of the whole record, subfigure (b), is rather smooth functions and is relatively well characterized by equation 6. This is present in all horizontal records. The higher amplitudes are concentrated around 7 to 9 seconds after the first amplitude of 0.05g in Arica and 15 to 19 seconds later, in Moquegua. This duration is larger for the Moquegua records. The strong energy arrival time agrees well with the expected arrival derived from the record analyses from broad band instruments at teleseismic distances.

The total record horizontal energy of the Arica Hospital record has a relatively rapid growth of approximately 40% of the total energy in less than 5 seconds. Nevertheless the bracket duration is in the order of 22 seconds and the strong motion duration according to Arias Intensity is around 24 seconds. The vertical record shows larger strong motion duration, 25 seconds.

Subfigure c and Figure 9 presents the energy distribution for each scale for all the records. It is important to notice that each scale is related to a non-constant frequency band. For horizontal records more than 90% of the energy lies in a band between 0.78 and 12 Hz, which corresponds to scales 4 to 7. The highest energy between 0.78 and 6 Hz is consistent with central frequency values. The Arica Hospital record presents most of its energy between 3 and 6 Hz. For the Moquegua records the highest energy is between 0.78 and 1.56 Hz. For vertical records most of the energy is found between 3.1 and 12.5 Hz in Chile, but the Moquegua records present much higher frequencies 12.5 to 25 Hz. Records in Poconchile and Putre that are relatively farther away, present single predominant bands with a maximum of 55% of the total energy of the record.

The evolution in time of the energy by scales in the horizontal records is presented in subfigure (d). They show that the lower frequency bands generally present jumps of energy in contrast with higher frequencies that show a more uniform presence in the record. Also, in general, the lower frequency energy is present in relatively shorter durations. This can be more easily appreciated when the mean and standard deviation of the energy evolution for each scale is compared to the mean time and standard deviation of the record. In figure 10 the scale mean time/record mean time ratio is presented for all horizontal and vertical records in the frequency band with more than 10% of energy. In general, we can realize that the time mean of each scale

does not change by more than 20% and in general, the higher values tend to grow with higher scales. The important parameter is that the ratios of the standard deviations of the scale envelope are smaller for the higher frequency bands for both horizontal and vertical records, i.e. the total energy is obtained on a longer duration of motion. The scale standard deviation ratios vary from 1.2 times, for the higher frequencies, i.e. longer duration, to 0.6 for the lower frequencies, shorter duration than the one obtained for the whole record.

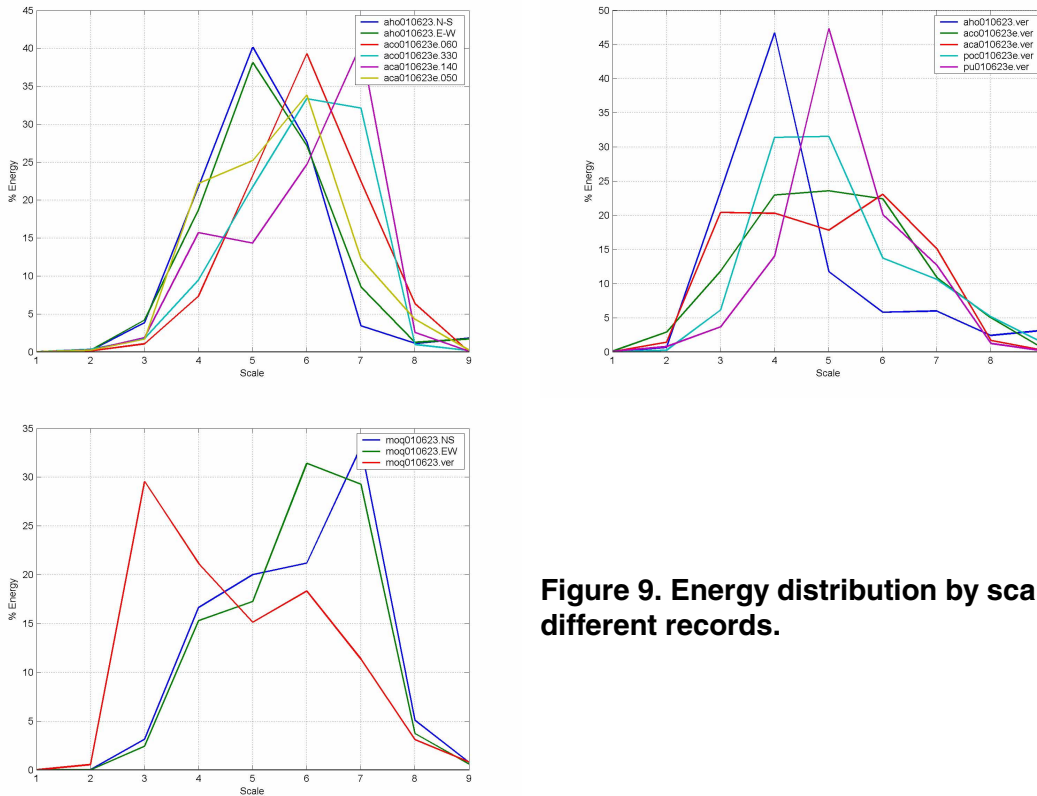


Figure 9. Energy distribution by scale in different records.

CONCLUSION

One of the most important earthquake events has been recorded for a subduction zone. Despite the relative long distance to the rupture and epicenter, important characteristics are observed.

The records confirm the relatively high central frequency of the subduction records of the Peruvian and Chilean region with horizontal frequencies of 3. to 4.8 Hz and vertical frequencies from 4.5 to 9.5 Hz. These records present relative large amplitude accelerations but relative lower maximum velocities due to these frequency characteristics.

The evolution of energy for the records and scales indicate that in general they can be modeled with a rather smooth parametric function with some possible refinement on the lower-frequency scales. In addition, generally the record envelope could be applied to the individual scales but with shorter duration for longer period scales.

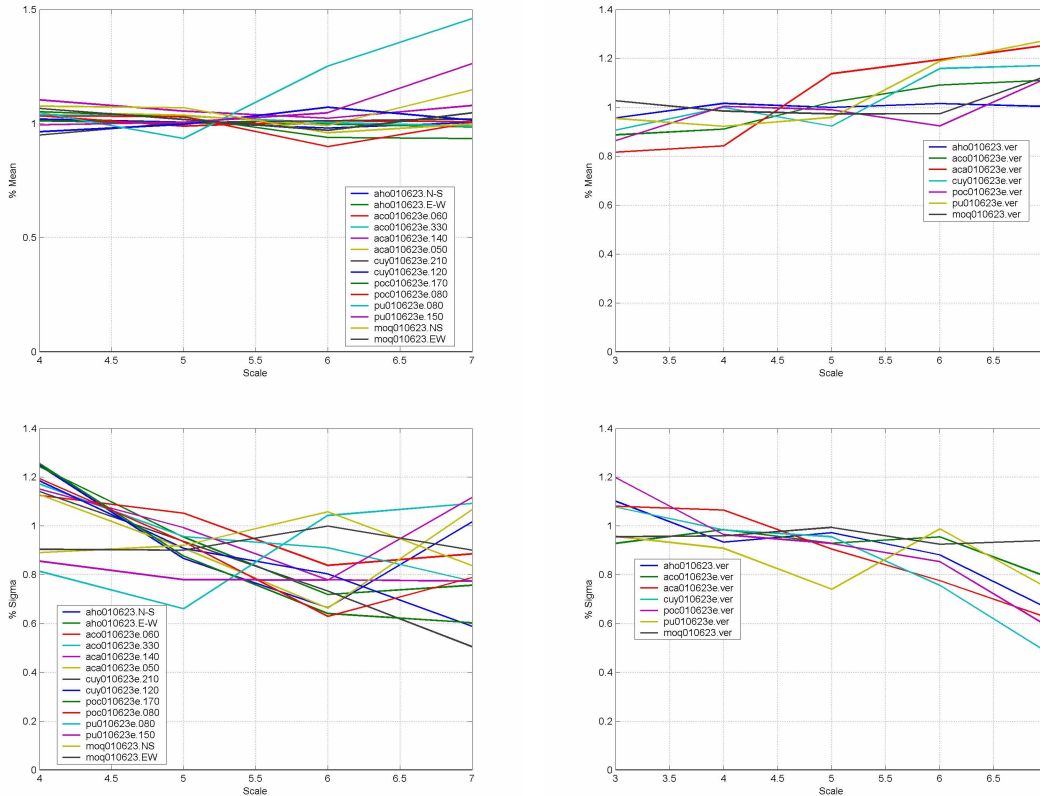


Figure 10. Scale/record ratio of time mean and standard deviation.

ACKNOWLEDGEMENT

The Chilean Council for Science and Technology, Conicyt, supported this research paper, Project FONDECYT 1000912 and partially funded by Project FONDECYT 1020104.

REFERENCES

1. Dorbath, L., Cisternas, A., Dorbath, C., "Assessment of the size of large and great historical earthquakes in Peru", *Bull. Seism. Soc. Am.*, 80, 551-576, 1990.
2. Nishenko, S., "Seismic potential for large and great interplate earthquakes along the Chilean and Southern Peruvian margins of South America: A quantitative reappraisal", *J. Geophys. Res.*, 90, 3589-3615, 1985.
3. Comte, D. y Pardo, M., "Reappraisal of great historical earthquakes in the northern Chile and southern Peru seismic gaps". *Natural Hazards*, 4, 23-44.1991
4. Giovanni, M., Beck, S., Wagner, L., "The June 23, 2001, Peru earthquake and the southern Peru subduction zone", American Geophysical Union Fall Meeting, San Francisco, Ca.-USA., *EOS*, 2001.

5. Kikuchi, M. And Yamanaka, Y., EIC Seismological Note N°105, Earthquake Information Center, University of Tokyo, 2001.
6. Nettles, M., Antolik, M., Ekstrom, G., and Dziewonski, A., “Long-period source characteristics of the June 23, 2001 Peru earthquake”, American Geophysical Union Fall Meeting, San Francisco, Ca.-USA., *EOS*, 2001.
7. Sladen, A., and Madariaga, R., “Nonlinear inversion of body waveforms of the June 2001 earthquakes in southern Peru”, American Geophysical Union Fall Meeting, San Francisco, Ca.-USA., *EOS*, 2002.
8. Boroschek, R, Soto, P, León, R. Record from Northern Chile: South of Peru Earthquake: June 23, 2001, Mw=8.4. (In Spanish: “Registros en el Norte de Chile: Terremoto del Sur del Peru, 23 de Junio de 2001, Mw=8.4). National Strong Motion Network, University of Chile, Report RENADIC 01-04, October 2001. (www.renadic.cl/red_archivos/SMA0107.pdf)
9. Boroschek, R., Comte, D., Morales, A. “Characteristics of the Ocoña Earthquake of June 23, 2001”. (In Spanish: “Características del Terremoto de Ocoña del 23 de Junio de 2001”). VIII Chilean Seminar on Seismology and Earthquake Engineering, Chile 2002.
10. Comte, D., Boroschek, R., Tavera, H, Dorbath, L., Portugal, D., Frogneux, M., Haessler, H., Montes, H., Bernal, I., Antayhua, Y., Salas, H., Inza, A., Rodríguez, S., Glass, B., Correa, E., Meneses, C., Balmaceda, I., Cruz, A., “Analysis of the South of Peru earthquake, June 23, 2001, Mw = 8.4 using local data”. (In Spanish: Análisis del terremoto del sur del Perú, 23 de Junio 2001, Mw=8.4 utilizando datos locales"). VIII Chilean Seminar on Seismology and Earthquake Engineering, Chile 2002.
11. Mallat, S. “A Wavelet Tour of Signal Processing”. Academic Press, Second edition, (1999).
12. Cohen, L. “Time-Frequency Analysis ”, Prentice Hall, First edition, (1995).
13. Boroschek, R. L., Szczecinski, L., Correa, D., Rivas, R. “Detection of time frequency characteristics in real earthquake records”, 2° Iberoamerican Congress of Earthquake Engineering, Madrid, 2002.
14. Saragoni, G. R, “Nonstationary Characterization and Simulation of Earthquake Ground Motions”, Ph. D. Dissertation, UCLA, Los Angeles, California, (1972).